

~~CONFIDENTIAL~~

Copy 6
RM E55BO8

NACA RM E55BO8



RESEARCH MEMORANDUM

CORRELATION OF TURBINE-BLADE-ELEMENT LOSSES BASED ON
WAKE MOMENTUM THICKNESS WITH DIFFUSION PARAMETER
FOR A SERIES OF SUBSONIC TURBINE BLADES IN
TWO-DIMENSIONAL CASCADE AND FOR FOUR
TRANSONIC TURBINE ROTORS

By Robert Y. Wong and Warner L. Stewart

CLASSIFICATION CHANGED

Lewis Flight Propulsion Laboratory
Cleveland, Ohio

UNCLASSIFIED

LIBRARY COPY

APR 25 1955

LANGLEY AERONAUTICAL LABORATORY
LIBRARY, NACA
LANGLEY FIELD, VIRGINIA

To _____

By authority of NACA Recall
+ RN-125

Date effective
Feb. 26, 1958
CLASSIFIED DOCUMENT

Amr 3-20-58

This material contains information affecting the National Defense of the United States within the meaning of the espionage laws, Title 18, U.S.C., Secs. 793 and 794, the transmission or revelation of which in any manner to an unauthorized person is prohibited by law.

NATIONAL ADVISORY COMMITTEE FOR AERONAUTICS

WASHINGTON

April 21, 1955

~~CONFIDENTIAL~~

NATIONAL ADVISORY COMMITTEE FOR AERONAUTICS

RESEARCH MEMORANDUM

CORRELATION OF TURBINE-BLADE-ELEMENT LOSSES BASED ON WAKE MOMENTUM

THICKNESS WITH DIFFUSION PARAMETER FOR A SERIES OF

SUBSONIC TURBINE BLADES IN TWO-DIMENSIONAL

CASCADE AND FOR FOUR TRANSONIC

TURBINE ROTORS

By Robert Y. Wong and Warner L. Stewart

SUMMARY

The analysis of losses occurring in a series of subsonic turbine blades in a low-speed two-dimensional cascade and in a related series of four transonic rotors is presented herein. The two-dimensional profile losses of turbine blades operating in the two-dimensional cascade over a wide range of incidence angle, stagger angle, inlet flow angle, and reaction could be generalized into one loss correlation curve when wake momentum thickness-to-chord ratio and suction-surface diffusion were used as parameters. A correlation of these losses on the basis of a loss parameter directly related to a product of wake momentum thickness-to-chord ratio and a function involving wake-form terms exhibited trends identical to the loss correlation based on wake momentum thickness. It was also indicated that the ratio of wake momentum thickness to suction-surface length for turbine loss correlations is preferable to a parameter based on the chord length, as used in compressor loss correlations. The indicated blade-element loss parameters at the hub, mean, and tip radius for a related series of transonic turbine rotors varied with diffusion parameters in a manner similar to that found for the two-dimensional loss correlations. A considerable difference was also found between the levels of the low-speed loss-correlation curve and the transonic turbine loss-correlation curves. From an analysis at zero diffusion, it was indicated that unsteady-flow effects on probe measurements and the effects of stator mixing losses can considerably influence the indicated rotor-blade-element losses. It was further indicated that about four-fifths of the true rotor-blade-element loss is attributable to compressible-flow profile loss, while the remainder is attributable to rotor three-dimensional and other effects.

INTRODUCTION

Analyzing and predicting blade-element losses in turbomachines have been severely hampered by the large number of variables that must be accounted for and the inability to obtain accurately the performance of a rotating blade element because of the complex three-dimensional nature of the flow. These three-dimensional effects act on the boundary-layer fluids to shift them from their section of origin to others at which they are measured, thus making difficult the evaluation of blade-element performance.

A significant step toward reducing the number of important variables in the correlation of two-dimensional compressor losses was made in unpublished data compiled at the NACA Lewis laboratory by Lieblein in which the blade wake momentum thickness and the velocity deceleration or diffusion on the suction surface of the blade were used as a basis for the correlation parameters. The use of these parameters generalizes compressor loss correlations, making them independent of solidity and outlet-flow angle. The hypothesis behind the use of these parameters is that the suction-surface boundary layer contributes a major portion of the low-momentum fluids that make up the wake of a blade. Since the velocity deceleration or diffusion on the suction surface of the compressor blade occurs over most of this surface, it probably is the main factor in determining the size of the suction-surface boundary layer and therefore the total wake thickness at the blade trailing edge. It can also be shown for two-dimensional incompressible flow through a cascade row that the wake momentum thickness-to-chord ratio is related to the mass-averaged total-pressure loss in the form given by equation (10) of reference 1. In the unpublished work of Lieblein, the wake momentum thickness-to-chord ratio was used as the basic measure of wake thickness or loss in order that the loss correlation be based completely on boundary-layer parameters.

Since turbine blades can differ markedly from compressor blades in both geometry and surface velocity distributions, it was considered of interest to determine if correlation parameters based on the deceleration of local suction-surface velocity and wake momentum thickness would be equally successful in generalizing turbine losses. In general, turbine blades differ from compressor blades as a result of the flow through a turbine blade row being required to turn through a much greater angle than that required through a compressor blade row. This requirement results in turbine blade designs that have higher camber angles, higher solidities, higher blade loading, and higher inlet and outlet flow angles. These effects can not only make the geometry of the turbine blade differ from compressor blades but can also affect the local surface velocity distribution around the blade. The surface velocity distribution around the blade for a given blade loading is also dependent upon

the amount and distribution of reaction across the blade row. Since the reaction across turbine blade rows varies over a considerably wider range than compressor blade rows, it is evident that for a given loading of the turbine blade the velocity deceleration or diffusion on the suction surface and the blade-surface length over which the diffusion takes place can vary over a considerable range.

Recent investigations of four transonic turbines (refs. 2 to 5) indicate that suction-surface diffusion is an important factor to be considered in the control of over-all turbine losses. A comparison of the experimentally obtained design-point efficiency among the four turbines (ref. 4) indicated that increased diffusion parameter was accompanied by a gradual increase in average blade loss (as indicated by over-all turbine efficiency) until a spanwise averaged diffusion parameter (obtained from the design procedure as in ref. 3) of 0.24 was reached. For diffusion parameters above 0.24, a sharp rise in average blade loss was indicated by the over-all turbine efficiency. General validity could not be inferred for loss correlations based on over-all turbine efficiency because of the large number of variables involved. Rotor-blade-element loss correlations in terms of parameters based on measured values of wake momentum thickness and suction-surface diffusion are impossible at present because instrumentation limitations prevent the measurements of the total-pressure distributions across rotating blade wakes and of the local surface velocity distribution around rotating blade rows. The problem of correlating turbine rotor losses can then be resolved into one of determining from two-dimensional turbine cascade data the significant parameters for generalizing turbine loss correlations, and one of approximating these parameters for turbine rotors to determine whether these parameters can be of significance in the correlation of turbine rotor-blade-element losses.

The object of this investigation is then twofold: (1) to determine from available two-dimensional turbine cascade loss data whether parameters based on wake momentum thickness and suction-surface diffusion will generalize two-dimensional turbine cascade losses as was done for two-dimensional compressor cascade losses, and (2) to approximate the wake momentum thickness parameter from the relative total-pressure loss for available turbines where the suction-surface diffusion parameter can also be readily approximated in order to determine if these parameters will also generalize measured turbine rotor-blade-element losses.

The first objective will be restricted to the loss data reported in reference 6, in which sufficient data are presented to calculate both the wake momentum thickness-to-chord ratio and the suction-surface diffusion parameter D . The second objective will be restricted to four transonic turbines operating only at design point (refs. 2 to 5), for which the blade-element diffusion parameters were obtained from the

3496

CW-1 back

design procedure. Although these restrictions may seem severe, it was felt that the results of the first objective of this investigation would not be affected by the restriction imposed, since the blades investigated in reference 6 appear to be representative of subsonic turbine blades, and the blades were operated over a representative range of conditions. The rotor loss correlations were necessarily restricted to turbines where the diffusion parameter could be obtained.

The approximation of wake momentum thickness-to-chord ratio was also calculated from the two-dimensional turbine cascade data in order to determine the effect of the use of the approximate loss parameter on the trend of loss correlations. Comparisons between the two-dimensional losses and the transonic turbine rotor losses are made in order to indicate what factors may be important in evaluating measured turbine rotor-blade-element losses.

DESCRIPTION OF BLADING

Two-Dimensional Cascade Blading

The loss data reported in reference 6 were obtained from operating the turbine blade profiles shown in figure 1 in a two-dimensional low-air-speed cascade. As can be seen in figure 1, the five blade profiles appear to be representative of subsonic turbine blades. The blade camber angle θ_c varied from 65° to 120° and the maximum thickness-to-chord ratio t/c varied from 10 to 25 percent. The table in figure 1 summarizes the range of inlet-air flow angle, solidity, and angle of attack covered in the investigation of reference 6. The pressure-coefficient curves given in reference 6 indicate that the range of reaction covered extends from approximately zero to highly positive. The range of incidence angle extends from highly positive to slightly negative.

Transonic Turbine Rotor Blading

Blade-element losses for the four transonic turbine rotors were obtained from radial and circumferential surveys made just downstream of the rotor operating at design point. The mean rotor-blade-element profiles forming the mean radius flow passages of the four transonic turbines are shown in figure 2, together with a table summarizing the important design features of each turbine. Angle surveys indicated that all blade elements of the four transonic turbines with the exception of the tip region of turbine IV were operated at approximately design incidence angle, which was about 4° . Surveys in the region of the tip of turbine IV indicated a positive angle of incidence of about 12° . The

design reaction across the rotors varied from negative at the hub of turbine IV to impulse at the hub of the other turbines, while the mean and tip sections were designed for positive reaction. The camber angle of the mean section of all four turbines is about 80°.

CALCULATION PROCEDURE

Two-Dimensional Cascade Loss-Correlation Parameters

The wake momentum thickness-to-chord ratio θ/c was calculated directly from the wake momentum difference coefficient $C_{w,1}$ and the inlet and outlet flow angles β_1 and β_2 , respectively, given in reference 6 by using an unpublished relation developed for two-dimensional incompressible flow by Lieblein as follows (symbols are defined in appendix A):

By definition,

$$C_{w,1} = \frac{\int_0^s \rho_2 V_{z,1,2} (V_{fs,2} - V_{l,2}) ds}{c \frac{1}{2} \rho_1 V_1^2} \quad (1)$$

For incompressible flow,

$$\rho_1 = \rho_2, \quad V_{z,1} = V_{z,2}, \quad \text{and} \quad \begin{cases} V_{z,2} = V_2 \cos \beta_2 \\ V_{z,1} = V_1 \cos \beta_1 \end{cases}$$

Substituting into equation (1) and rearranging gives

$$C_{w,1} = \frac{2}{c} \left(\frac{\cos \beta_1}{\cos \beta_2} \right)^2 \cos \beta_2 \int_0^s \frac{V_{l,2}}{V_{fs,2}} \left(1 - \frac{V_{l,2}}{V_{fs,2}} \right) ds \quad (2)$$

By definition,

$$\theta = \cos \beta_2 \int_0^s \frac{V_{l,2}}{V_{fs,2}} \left(1 - \frac{V_{l,2}}{V_{fs,2}} \right) ds \quad (3)$$

where θ is measured in a direction normal to the direction of flow. By substituting equation (3) into equation (2) and rearranging,

$$\frac{\theta}{c} = \frac{C_{w,1}}{2} \left(\frac{\cos \beta_2}{\cos \beta_1} \right)^2 \quad (4)$$

is obtained.

Also, the approximation of the wake momentum thickness-to-chord ratio was calculated from

$$\frac{\bar{\omega}_2 \cos \beta_2}{\sigma} = \frac{C_{D,1}}{\cos \beta_m} \frac{S_1}{S_2} \cos \beta_2$$

using the required quantities given in reference 6 (see appendix B for the derivation of this equation). The term $\frac{\bar{\omega}_2 \cos \beta_2}{\sigma}$, herein designated as the loss parameter, has been found to be related to the wake momentum thickness-to-chord ratio by terms involving the wake form. Also, the effect of the form terms on the relation between the total-pressure loss and the wake momentum thickness is of the second order.

A suction-surface diffusion parameter D , defined as the difference between the maximum suction-surface relative velocity and blade outlet relative velocity divided by the maximum suction-surface relative velocity, was calculated using the relation

$$D = 1 - \sqrt{\frac{S_{max}}{S_2}}$$

and the pressure coefficients S given in reference 6.

Transonic Turbine Loss-Correlation Parameters

Rotor-blade-element loss parameters for the hub, mean, and tip sections were calculated from radial and circumferential surveys of total pressure, total temperature, and flow angle taken at design-point operation of each turbine previously investigated in references 2 to 5. The rotor-blade-element loss parameter was calculated from

$$\frac{\bar{\omega}_2 \cos \beta_2}{\sigma} = \frac{\left[1 - \left(\frac{p_2'}{p_1'} \right) \left(\frac{T_1'}{T_2'} \right)^{\frac{\gamma}{\gamma-1}} \right] \frac{\cos \beta_2}{\sigma}}{\left(\frac{p_2'}{p_1'} \right) \left(\frac{T_1'}{T_2'} \right)^{\frac{\gamma}{\gamma-1}} - \frac{p_2}{p_1' \left(1 - \frac{\gamma-1}{\gamma+1} \frac{2v_{u,1} U_1 - U_1^2}{v_{cr,1}^2} \right)^{\frac{\gamma}{\gamma-1}}}}$$

developed in appendix C using local values of total pressure and total temperature corrected for probe recovery factor, outlet relative flow angle, a calculated inlet velocity diagram, and measured outlet static pressure.

The local values of turbine-outlet total pressure, total temperature, and flow angle used in the loss calculation were selected in a manner such that the direct effect of stator wakes would be minimized, and thus a better indication of rotor-blade-element losses would be obtained. This was accomplished by selecting peak values of local adiabatic efficiency from a circumferential survey at any given radial station. The hypothesis behind this selection is that stator losses in passing through the rotor cause patterns in the contours of local adiabatic efficiency which have been identified as the effects of stator losses (ref. 7). Specifically, the regions of low efficiency are made up of stream particles flowing along streamlines emanating from the stator wakes and loss regions, whereas the regions of high efficiency are made of stream particles moving along streamlines emanating from regions of free-stream flow through the stator blade row. As the stream particles pass downstream of the stator, the kinetic energy level of the stream particles emanating from the wake regions will rise, whereas the kinetic energy level of the stream particles emanating from the free-stream flow regions of the stator will fall as a result of mixing. In addition to this mixing effect, there is an additional loss in the kinetic-energy level of all stream particles directly due to the mixing itself. As the rotor blades pass through each streamline, the rotor losses are superimposed on each streamline. Therefore, the selection of points corresponding to streamlines emanating from the regions of free-stream stator flow, namely the peak values of local adiabatic efficiency, tends to minimize the effects of stator losses on the measured rotor-blade-element losses. It must be noted, however, that the selection of the peak-efficiency points does not completely exclude the effects of stator losses because of mixing effects, and the stator losses may induce appreciable losses

on the rotor blades because of time unsteady effects. Plotted in figure 3 against radius ratio are the maximum and minimum local adiabatic efficiencies at any given radius. The curves illustrate the stator effects that are superimposed on the local efficiencies as previously discussed. As can be seen from figure 3, the point selected for the mean-section loss calculation is near the mean-radius section where a data point was available. For the hub and tip sections, data points corresponding to approximately the peak efficiency of the faired curves were selected from a region covering 15 percent of the blade span from either wall in order to assure selecting a point where end wall effects would not predominate.

The diffusion parameter D was calculated from the blade surface velocity distributions obtained in the design procedure (refs. 2 to 5). Although the exact value of diffusion parameter obtained by this method may be questionable, it is felt that these values are indicative of the differences in diffusion parameter obtained among the four turbines operating at design point, because the design procedure has been successfully used in the design of turbines that are highly critical with respect to limiting loading.

RESULTS AND DISCUSSION

Two-Dimensional Cascade Loss Correlations

The results obtained from making calculations as outlined in CALCULATION PROCEDURE on the two-dimensional low-speed loss results of reference 6 are shown in figure 4, in which wake momentum thickness-to-chord ratio θ/c and loss parameter $\frac{\omega_2 \cos \beta_2}{\sigma}$ are plotted against suction-surface diffusion parameter D . Comparison of these loss curves indicates that the general trends of losses based on either parameter are similar, thus indicating that the form factor has only a second-order effect on the relation between wake momentum thickness and total-pressure loss.

It was also observed that the trend of loss based on either parameter with diffusion parameter is similar to that found in the unpublished compressor data except for the tailed points. These points were loss results from the highly cambered blades ($\theta_c = 110^\circ$ and 120°) operating at inlet flow angles β_1 of 45° and 60° , respectively. The blade loss based on either parameter for these blades rises sharply with increased diffusion parameter, whereas there is gradual rise in blade loss with increased diffusion for the other blades.

An inspection of the surface velocity distribution as indicated by the pressure-coefficient curves given for these blades in figures 18 and 30 of reference 6 indicated that there are two possible reasons for the lack of correlation for these blades. At angles of attack α_1 near and below the design value, the initial surface deceleration of the flow at the leading-edge portion of the pressure surface of the blade was followed by alternate acceleration and deceleration. At angles of attack above the design value, a similar situation exists on the suction surface of the blade where the initial surface acceleration was followed by alternate deceleration and acceleration. It is well known that local phenomena of this nature can have considerable influence on the local boundary-layer growth and hence affect the final loss. Therefore, in the cases where the alternate acceleration and deceleration on either surface is severe, it is unlikely that blade losses based on wake characteristics would correlate with suction-surface diffusion parameter, since these effects may have considerable effect on the blade loss.

Another factor that may contribute to the lack of correlation for the highly cambered blades is that the chord length of these blades is not representative of the surface length over which the flow must travel (wetted surface area per unit blade height). Thus, it may be expected that the use of suction-surface length in the blade-loss parameter would be more accurate for highly cambered blades. The losses for the blade profiles presented in reference 6 were therefore recalculated on the basis of the ratio of the wake momentum thickness to the suction-surface length θ/l_s and plotted against diffusion parameter D in figure 5. Comparison of figures 4(a) and 5 indicates that the loss correlation, in general, was slightly improved by basing the loss parameter on suction-surface length instead of chord length. Furthermore, it can be seen that correlation for the highly cambered blades is also improved; however, these points do not yet line up with points obtained for the other blades. Hence, the lack of correlation on this basis may be attributed to increased losses on the pressure surface or to the effects of double diffusion on the suction surface, as discussed in the previous paragraph.

The loss correlation curves in figure 4 established a criterion for losses occurring in low-speed two-dimensional turbine cascade blade rows. However, the curves are obtained from low-speed results, and their validity for high speed has not been established. On the basis of the work done on the effect of increased airspeeds on compressor blade losses (ref. 8, e.g.), it appears that the level of losses in figure 4 is low compared with the losses that would occur if the turbine blades of reference 6 were operated at transonic airspeeds. Another indication of this speed effect was obtained from the limited high-speed tests conducted in reference 6 on two of the blade profiles at

outlet Mach numbers up to 0.9. Calculations of these high-speed loss results on the basis of wake momentum thickness-to-chord ratio are plotted against diffusion parameter in figure 6. The low-speed results are also shown in the figure, which indicates that increased airspeeds tended to increase the profile losses. The high-speed results tend to fall along the high range of the spread of the low-speed data. No definite trends appear to have been established with these high-speed results, since they fall within the spread of the low-speed results, thus indicating that shock losses were not too severe for these high-speed tests.

Transonic Turbine Loss Correlations

The results of loss calculations made on the survey results obtained from the four transonic turbine rotors operated at design point are plotted in terms of the loss parameter $\frac{\overline{\omega}_2 \cos \beta_2}{\sigma}$ against the design value of diffusion parameter D in figure 7 for the hub-, mean-, and tip-radius blade elements. These curves show that the measured rotor-blade-element loss parameter is related to diffusion parameter in a manner similar to that found for turbine blades in the low-speed two-dimensional cascade with the exception of the tip radius, where a sharp rise in the measured blade-element loss parameter occurred as the diffusion parameter was increased above 0.24. It is further noted that the magnitudes of the loss parameter measured at the hub and mean radius are of comparable levels, while the magnitude of the tip-radius loss parameters is about twice that at the other two sections, thus, indicating that rotor three-dimensional effects may have considerable effect on the magnitude of the measured rotor losses.

Comparison of the measured transonic turbine losses (fig. 7) with the low-speed cascade losses (fig. 4(b)) indicates that the transonic turbine rotor-blade-element losses are considerably greater than the low-speed cascade losses. Specifically, a comparison of the loss parameters at a diffusion parameter of zero in figures 4(b) and 7(b) indicates that the low-speed cascade loss is less than 10 percent of that measured at the mean section of the zero diffusion turbine (turbine I). The following discussion considers some of the important factors that must be considered in the evaluation of blade-element losses measured behind a turbine rotor by using the loss parameter measured at the mean radius of turbine I as an example.

Effect of Unsteady Flows

It is well known that unsteady flow fields such as those existing behind rotating blade rows can have considerable effect upon the total-pressure and total-temperature measurements taken within these fields,

and thus influence the relative total-pressure loss across the rotor blade row as indicated by these measurements. In order to obtain an insight as to the order of magnitude of the effect of these unsteady flow fields on the measured losses of turbine I, a comparison was made between the turbine relative total-pressure ratio calculated from equation (C3) of appendix C using (1) the mass-averaged survey values of total temperature and total pressure, and (2) measurements of torque, turbine speed, weight flow, outlet flow angle, and outlet static pressure obtained in the over-all performance investigation at identical operating conditions (ref. 2). The relative total-pressure ratio based on the performance investigation is considered to be the more accurate of the two, since it is not affected by the unsteady flow fields. The difference in the two relative total-pressure ratios may be used to indicate the errors due to the unsteady flow effects.

In order to evaluate any difference in the turbine relative total-pressure ratio as obtained from the two sets of instrumentation, consideration must be given to the fact that the turbine relative total-pressure ratio based on performance results includes the total-pressure loss due to the mixing of the rotor-blade wakes, whereas the survey results were taken so close behind the trailing edge of the rotor that little total-pressure loss due to mixing of the rotor blade wakes is included in the survey measurements. The method by which the differences in the two rating methods were calculated is given in appendix D. A comparison of the turbine relative total-pressure ratio obtained from the survey results to the performance value of the turbine relative total-pressure ratio (corrected for a theoretical rotor wake mixing loss) gave the error induced by unsteady-flow effects in terms of a fictitious total-pressure ratio that was applied to the local measured rotor-blade-element loss. The application of this fictitious total-pressure ratio to the losses measured at the mean radius of turbine I indicates that the actual loss occurring along a streamline emanating from the regions of free-stream flow through the stator is only 49 percent of that indicated by the survey measurements.

Mixing of Stator Wakes

The actual loss occurring along the selected streamline indicated by the previous section is the sum of the stator losses that have not been excluded by the calculation procedure and losses induced by the rotor as the rotor blades pass through the streamline. In order to obtain an indication as to the true level of the rotor-induced losses at the mean radius of turbine I, it is necessary to obtain an indication of the order of magnitude of the mixing effect of the stator blade wakes.

The effects of mixing of blades wakes on the losses measured along a streamline are twofold. First, there is an exchange of momentum between

the free-stream regions of flow and the wake regions of flow (often referred to as mixing). Second, as a result of this momentum exchange, there is a further loss in momentum or total pressure in both regions. Their combined effect on the local losses measured at the exit of turbine I could not be measured directly since it was found in reference 9 that without the rotor in place almost complete mixing of these stator wakes occurred in an axial distance corresponding to approximately the rotor axial chord. With the rotor in place, only partial mixing of the stator wakes has taken place, because the stator wakes still appear in the total-pressure surveys taken at the same axial station. In reference 9 it was also found that without the rotor in place complete mixing of the wakes in these stators resulted in a 1.5 percent additional loss in the inlet total pressure at the mean radius. With the rotor in place, however, the additional total-pressure loss due to mixing is probably not as great as the 1.5 percent found in reference 9; however, it is believed that the loss resulting from the combined effects of the momentum exchange as discussed previously may approach a value of 1.5 percent of the inlet total pressure of turbine I. When this value of loss was used as a criterion for the combined effects of stator-wake mixing it was found that the measured local loss of turbine I was affected by about 20 percent.

Correction of the measured mean-radius blade-element losses of turbine I for the effects of unsteady flow fields and for the losses due to mixing of the stator wakes showed that the true mean-radius rotor-blade-element loss for turbine I was considerably less than that indicated by the survey instrumentation. Plotted in figure 8 is the measured mean-radius blade-element loss for turbine I as a ratio of the true mean-radius blade-element loss. Shown also in figure 8 in terms of the true blade-element loss is the breakdown of the effects that unsteady flow fields and mixing of stator wakes had on the indicated mean-radius blade-element loss of turbine I.

Compressibility. - In order to obtain an indication as to the effect of transonic airspeeds on profile losses in a turbine blade row, the total-pressure loss measured across the mean section of the stator used in the transonic turbine investigations was mass averaged and found to be about three times the loss indicated by the low-speed turbine cascade loss correlations at zero diffusion (fig. 5). An analysis of the surface velocity distribution of these blades by the method given in reference 3 indicates that the suction-surface diffusion parameter for these stators is zero. The loss parameter found for the stator mean section can then be assumed to be approximately equal to the loss parameter corresponding to the compressible-flow profile loss of the rotor mean section of turbine I, since the two-dimensional loss correlations presented in figures 4(a) and 4(b) are independent of blade shape, and both blades sections are operating at comparable Mach number levels and at zero diffusion. This value of loss parameter was plotted in figure 8 and labeled compressible-flow profile loss to illustrate the order of magnitude of

the profile losses as compared with the true loss. From figure 8, it can be seen that the profile loss is estimated to be of the order of 81 percent of the true rotor-blade-element loss. The low-speed profile loss is shown in figure 8 (dashed line) in order to emphasize the difference in loss levels.

Three-dimensional effects. - It has been found by various investigators that three-dimensional effects tend to shift boundary-layer fluids radially from one point to another. An inspection of the variation of maximum and minimum local efficiency with radius for the four transonic turbines given in figure 3 indicates that the efficiency level at the hub is generally higher than that at the tip. Furthermore, the level of efficiency measured at the hub is only slightly lower than that obtained in the highest efficiency regions. Thus, it appears that these three-dimensional effects are shifting considerable amounts of hub-wall losses onto the rotor-blade surfaces, thus increasing the efficiency measured in the region of the hub and decreasing the efficiency measured elsewhere, and in particular the tip-radius region.

Three-dimensional effects may then be the main contributor to the remaining loss in figure 8, which is the difference between the true mean-radius blade-element loss of turbine I and the compressible-profile loss estimated from the loss measured at the mean radius of the stators and amounts to about one-fifth the true loss. Further indications that rotor three-dimensional effects are important to turbine losses are seen in a comparison of the level of losses measured at the hub- and mean-radius regions with those at the tip-radius region (fig. 7). The level of loss at the tip-radius region (up to $D = 0.24$) is about twice that obtained at the hub and mean radius, and it appears that the increased losses at the tip are the effects of the radial transport of boundary-layer fluids in combination with the complex secondary flows occurring in the tip region.

The sharp rise in the loss curve above a diffusion parameter of 0.24 for the tip may be attributed to the diffusion parameter of turbine IV not being the value obtained in the design procedure, since surveys taken upstream of the rotor indicated approximately a positive 12° angle of incidence in the region of the tip of turbine IV at design-point operation. It is believed that the radial transport of boundary-layer fluids into the tip region of this turbine combined with losses originating in the tip region prematurely chokes this region, thus causing a mass-flow shift toward the hub at the rotor inlet, which, in turn, resulted in a positive angle of incidence at the tip. Since it is well known that increases in incidence angle tend to increase the loading of the suction surface, it can then be concluded that the actual diffusion parameter is larger than that obtained in design procedure, which, in turn, would tend to temper the sharp rise in the loss correlation curve of the tip by shifting the loss point to the right.

SUMMARY OF RESULTS

The analysis of losses occurring in a series of subsonic turbine blades in a low-speed two-dimensional cascade and in a related series of transonic turbines is presented herein. The pertinent results of this investigation are summarized as follows:

1. The profile losses of a related series of subsonic turbine blades in a two-dimensional cascade as measured by wake momentum thickness-to-chord ratio were found to correlate with diffusion parameter for a wide range of blade profile, incidence angle, stagger angle, and inlet flow angle. Correlation of these losses based on a loss parameter, which is directly related to a product of the wake momentum thickness-to-chord ratio and the wake-form terms was found to have trends identical to loss correlations based on wake momentum thickness. It was also indicated that the ratio of wake momentum thickness to suction-surface length is a preferable loss parameter to use in turbine-blade loss correlations.

2. The indicated blade-element loss parameters of a related series of transonic turbines varied with diffusion parameter in a manner similar to that found for the two-dimensional cascade losses.

3. A considerable difference in the loss levels between the two-dimensional and transonic turbine results was found. From an analysis at a diffusion parameter of zero, it was indicated that the effects of unsteady flow on total-temperature and total-pressure measurements and stator mixing loss can have considerable effect on the measured rotor-blade-element losses. It was further indicated that about four-fifths of the true rotor-blade-element loss is attributable to compressible-flow profile losses, while the remainder is attributable to rotor three-dimensional and other effects.

Lewis Flight Propulsion Laboratory
National Advisory Committee for Aeronautics
Cleveland, Ohio, February 10, 1955

APPENDIX A

SYMBOLS

The following symbols are used in this report:

| | |
|--------------------------------------|--|
| $C_{D,1}$ | drag coefficient |
| $C_{w,1}$ | wake momentum difference coefficient (see ref. 6) |
| c | chord length, ft |
| D | diffusion parameter defined as difference between maximum suction-surface relative velocity and outlet relative velocity divided by maximum suction-surface relative velocity |
| $f(H)$ | terms involving form of wake |
| l_s | suction-surface length, ft |
| p | absolute pressure, lb/sq ft |
| $\left(\frac{p_2''}{p_1''}\right)_p$ | turbine relative total-pressure ratio calculated from over-all measurements |
| $\left(\frac{p_2''}{p_1''}\right)_s$ | turbine relative total-pressure ratio calculated from mass-averaged survey values of total-temperature ratio and total-pressure ratio measured from turbine inlet to just downstream of trailing edge of rotor |
| r | radius, ft |
| S | pressure coefficient, $(p_1^i - p_2^i)/(p_1^i - p_1) = \frac{\frac{1}{2} \rho V_2^2}{\frac{1}{2} \rho V_1^2}$ |
| s | blade spacing or pitch, ft |
| T | absolute temperature, °R |
| t | blade thickness, ft |
| U | blade speed, ft/sec |
| V | absolute gas velocity, ft/sec |
| w | weight-flow rate, lb/sec |

- α angle of attack, measured from entering flow to chord
- β gas flow angle measured from axial direction, deg
- β_m vector mean gas flow angle between inlet and outlet flow angle, deg
- γ ratio of specific heats
- δ ratio of turbine inlet total pressure to NACA standard sea-level pressure, p'/p^*

ϵ function of $\gamma, \frac{\gamma^*}{\gamma} \frac{\left[\left(\frac{\gamma + 1}{2} \right)^{\frac{\gamma}{\gamma - 1}} \right]}{\left(\frac{\gamma^* + 1}{2} \right)^{\frac{\gamma^*}{\gamma^* - 1}}}$

- η_l local adiabatic efficiency based on local total-state measurements upstream of stator and downstream of rotor
- θ momentum thickness, ft
- θ_c blade camber angle, deg
- θ_{cr} squared ratio of critical velocity at turbine inlet to critical velocity at NACA standard sea-level temperature, $(V_{cr}/V^*_{cr})^2$
- ρ static density, lb/cu ft
- $\bar{\omega}_1$ relative total-pressure loss coefficient based on inlet dynamic head
- $\bar{\omega}_2$ relative total-pressure loss coefficient based on outlet dynamic head
- σ solidity, ratio of blade chord to pitch, c/s

Subscripts:

- cr condition at Mach number of unity
- fs free-stream conditions
- l local conditions

max local conditions corresponding to maximum value of pressure coefficient S

t tip

u tangential direction

z axial direction

1 conditions at inlet to a blade row

2 conditions at outlet of a blade row

Superscripts:

* NACA standard conditions

' absolute total state

" relative total state

APPENDIX B

DEVELOPMENT OF A LOSS PARAMETER AS AN APPROXIMATION OF WAKE MOMENTUM
THICKNESS PARAMETER AND CALCULATION OF THIS LOSS PARAMETER FROM
DRAG COEFFICIENT FOR STATIONARY BLADE ROWS

From unpublished NACA data, the total-pressure loss across a blade row mass averaged across a blade pitch is related to the wake momentum thickness by

$$\overline{\Delta p^t} = \frac{1}{2} \rho_2 V_2^2 \frac{\frac{\theta}{c} \sigma}{\cos \beta_2} [f(H)] \quad (B1)$$

For incompressible flow, the term involving the form of the wake $f(H)$ has been found to have only a second-order effect on the relation between total-pressure loss and wake momentum thickness, and hence may be assumed constant. Since, by definition,

$$\overline{\omega}_2 = \frac{\overline{\Delta p^t}}{\frac{1}{2} \rho_2 V_2^2}$$

equation (B1) may be rewritten as follows:

$$\frac{\overline{\omega}_2 \cos \beta_2}{\sigma} = \frac{\theta}{c} f(H) \quad (B2)$$

so that if the form term is assumed constant the wake momentum thickness-to-chord ratio will vary directly with the terms involving the total-pressure loss coefficient, the outlet flow angle, and the solidity of the blade row.

Loss correlations based on a loss parameter involving the terms on the left side of equation (B2) should exhibit loss trends that are similar to those based on wake momentum thickness-to-chord ratio. The loss parameter $\frac{\overline{\omega}_2 \cos \beta_2}{\sigma}$ was calculated from the low-speed two-dimensional cascade results of reference 6 by use of equation (B17) of reference 8, which restated is

$$\overline{\omega}_1 = \frac{\sigma C_{D,1}}{\cos \beta_m} = \frac{\overline{\Delta p^t}}{p_1' - p_1}$$

Since

$$\bar{\omega}_2 = \frac{\overline{\Delta p^i}}{p_1^i - p_1} \frac{p_1^i - p_1}{p_2^i - p_2}$$

then

$$\bar{\omega}_2 = \frac{\sigma C_{D,1}}{\cos \beta_m} \frac{p_1^i - p_1}{p_2^i - p_2}$$

From reference 6,

$$S_1 = \frac{p_1^i - p_1}{p_1^i - p_1} \quad \text{and} \quad S_2 = \frac{p_2^i - p_2}{p_1^i - p_1}$$

Substituting gives

$$\bar{\omega}_2 = \frac{\sigma C_{D,1}}{\cos \beta_m} \frac{S_1}{S_2}$$

Multiplying both sides by $\frac{\cos \beta_2}{\sigma}$, obtained from data supplied in reference 6, yields

$$\frac{\bar{\omega}_2 \cos \beta_2}{\sigma} = \frac{C_{D,1}}{\cos \beta_m} \frac{S_1}{S_2} \cos \beta_2 \quad (B3)$$

which was used to calculate the loss parameter for the two-dimensional low-speed results.

APPENDIX C

EQUATIONS AND ASSUMPTIONS MADE IN CALCULATING ROTOR-
BLADE-ELEMENT LOSS PARAMETER

Rotor-blade-element losses for the hub, mean, and tip sections were calculated in terms of a loss parameter $\frac{\bar{\omega}_2 \cos \beta_2}{\sigma}$ in the following manner: The relative total-pressure loss coefficient $\bar{\omega}_2$ was calculated from the equation

$$\bar{\omega}_2 = \frac{p_1'' - p_2''}{p_2'' - p_2}$$

Dividing both terms on the right side by p_1'' gives

$$\bar{\omega}_2 = \frac{1 - \frac{p_2''}{p_1''}}{\frac{p_2''}{p_1''} - \frac{p_2}{p_1}} \quad (C1)$$

The relative total-pressure ratio p_2''/p_1'' in equation (C1) can be evaluated from absolute measurements as follows:

$$\frac{p_2''}{p_1''} = \frac{p_2'}{p_1'} \cdot \frac{p_2''}{p_2'} \cdot \frac{p_1'}{p_1''}$$

From isentropic relations,

$$\frac{p_2''}{p_1''} = \frac{p_2'}{p_1'} \left(\frac{T_2''}{T_2'} \cdot \frac{T_1'}{T_1''} \right)^{\frac{\gamma}{\gamma-1}} \quad (C2)$$

It is assumed that

$$\frac{T_1''}{T_2''} = 1.00$$

Thus,

$$\frac{p_2''}{p_1''} = \frac{p_2'}{p_1'} \left(\frac{T_1'}{T_2'} \right)^{\frac{\gamma}{\gamma-1}} \quad (C3)$$

From this relation the relative total-pressure ratio may then be calculated from measured absolute values of total-pressure ratio and total-temperature ratio.

The static pressure downstream of the rotor p_2 and the inlet relative total pressure p_1'' in the denominator of the right term of equation (C1) were calculated independently of each other as follows: A linear variation between the outlet static pressure measured at the hub and tip is assumed in order to find p_2 at a given radial station. The inlet relative total pressure is calculated from measured values of absolute inlet total pressure, inlet total temperature, inlet absolute flow angle, and wheel speed by use of the equation

$$p_1'' = p_1' \left[1 - \frac{\gamma-1}{\gamma+1} \left(\frac{2v_{u,1}U_1 - U_1^2}{v_{cr,1}^2} \right)^{\frac{\gamma}{\gamma-1}} \right] \quad (C4)$$

Substituting equations (C4) and (C3) into equation (C1) and multiplying both sides by $\frac{\cos \beta_2}{\sigma}$ give the final relation for calculating the rotor-blade-element loss parameter:

$$\frac{\bar{\omega}_2 \cos \beta_2}{\sigma} = \frac{\left\{ 1 - \left[\left(\frac{p_2'}{p_1'} \right) \left(\frac{T_1'}{T_2'} \right)^{\frac{\gamma}{\gamma-1}} \right] \right\} \frac{\cos \beta_2}{\sigma}}{\left(\frac{p_2'}{p_1'} \right) \left(\frac{T_1'}{T_2'} \right)^{\frac{\gamma}{\gamma-1}} - \frac{p_2}{p_1' \left[1 - \frac{\gamma-1}{\gamma+1} \left(\frac{2v_{u,1}U_1 - U_1^2}{v_{cr,1}^2} \right)^{\frac{\gamma}{\gamma-1}} \right]}} \quad (C5)$$

APPENDIX D

METHOD OF EVALUATING EFFECTS OF UNSTEADY FLOWS ON MEASURED

BLADE-ELEMENT LOSSES

An evaluation of the effect of unsteady flows on the indicated blade-element losses for turbine I at design point can be obtained by comparing the turbine relative total-pressure ratio computed from equation (C3), using mass-averaged survey values of total-temperature and total-pressure ratios, with the turbine relative total-pressure ratio obtained at the same operating conditions but from measurements of torque, speed, weight flow, outlet flow angle, and rotor outlet static pressure, which were obtained in the over-all performance investigation (ref. 2). The turbine relative total-pressure ratio calculated from the mass-averaged survey results (p_2''/p_1'') _s was found to be 0.871, whereas the turbine relative total-pressure ratio calculated from the over-all performance results (p_2''/p_1'') _p was 0.885.

Since the value obtained from the over-all performance results is considered to be the more accurate of the two rating methods, it is evident that survey results indicate larger losses than those indicated by the over-all performance results. A direct comparison of the turbine relative total-pressure ratios obtained from the two methods cannot be made to evaluate the error induced by unsteady flows because the turbine relative total-pressure ratio calculated from the over-all performance results (p_2''/p_1'') _p includes the total-pressure loss due to mixing of the rotor-blade wakes. However, the turbine relative total-pressure ratio calculated from the mass-averaged survey results (p_2''/p_1'') _s does not include the mixing loss of the rotor wakes because the surveys were taken so close to the trailing edge of the rotor that little or no total-pressure loss due to mixing of the rotor wakes has occurred. In order to evaluate the effect of unsteady flows on the measured blade-element losses by comparison of the turbine relative total-pressure ratios, it is necessary to account for this difference in the rotor wake mixing loss between the two methods.

The rotor wake mixing loss can be accounted for by writing the turbine relative total-pressure ratio (p_2''/p_1'') _p in terms of its component losses, which are the product of the total-pressure ratios that correspond to the stator losses, mixing of stator wakes, relative rotor loss, and mixing of rotor wakes. Since the wake mixing loss was shown in reference 9 to be related directly to the total loss at the exit of

967C

the blade row, the various losses that make up the turbine relative total-pressure ratio (p_2''/p_1'') may be found from a knowledge of the

stator loss. The stator total-pressure ratio was determined from mass-averaged radial and circumferential surveys of total pressure just downstream of the trailing edge of the stator and was found to be 0.968. An over-all stator total-pressure ratio (product of the total-pressure ratio corresponding to the stator loss and mixing of stator losses) was found to be 0.950 from figure 4 in reference 9, which assumes linear variation in total pressure across the wake from free stream to the minimum total pressure and back to free stream. With these quantities, the rotor relative total-pressure ratio, including rotor wake mixing losses, was calculated from the turbine relative total-pressure ratio (p_2''/p_1'') and was found to be 0.932. The rotor relative total-pressure

ratio before mixing of the rotor wakes was also found from figure 4 in reference 9 to be 0.952, thus giving a value of 0.978 for the pressure ratio due to mixing of rotor wakes. Dividing the turbine relative total-pressure ratio (p_2''/p_1'') by the total-pressure ratio corresponding

to the rotor wake mixing loss gives a value of 0.905 for the turbine relative total-pressure ratio before mixing of the rotor wakes. If the turbine relative total-pressure ratio (p_2''/p_1'') is also written as a

product of the total-pressure ratios that corresponds to the stator losses, stator mixing losses, rotor relative total-pressure loss, and a fictitious loss to account for the effects due to unsteady flows, dividing (p_2''/p_1'') by (p_2''/p_1'') (before mixing of the rotor wakes)

gives the value of the fictitious pressure ratio that is included in the survey results because of the effects of unsteady flows. This fictitious pressure ratio was found to have a value of 0.962 for turbine I and was assumed to be representative of the errors induced in the survey results of turbine I.

The local relative total-pressure ratio obtained from the survey results at the mean radius of turbine I was divided by the fictitious total-pressure ratio to obtain a corrected value of the local relative total-pressure ratio. This corrected value was used to calculate a new loss parameter of 0.0254, which is about 49 percent of the loss parameter (0.0523) indicated by the survey results.

REFERENCES

1. MacGregor, Charles A.: Two-Dimensional Losses in Turbine Blades. Jour. Aero. Sci., vol. 19, no. 6, June 1952, pp. 404-408.

2. Whitney, Warren J., Monroe, Daniel E., and Wong, Robert Y.:
Investigation of Transonic Turbine Designed for Zero Diffusion of Suction-Surface Velocity. NACA RM E54F23, 1954.
3. Stewart, Warner L., Wong, Robert Y., and Evans, David G.:
Design and Experimental Investigation of Transonic Turbine with Slight Negative Reaction Across Rotor Hub. NACA RM E53L29a, 1954.
4. Whitney Warren J., Wong, Robert Y., and Monroe, Daniel E.: Investi-
gation of a Transonic Turbine Designed for a Maximum Rotor-Blade Suction-Surface Relative Mach Number of 1.57. NACA RM E54G27, 1954.
5. Wong, Robert Y., Monroe, Daniel E., and Wintucky, William T.:
Investigation of Effect of Increased Diffusion of Rotor-Blade Suction-Surface Velocity on Performance of Transonic Turbine. NACA RM E54F03, 1954.
6. Dunavant, James C., and Erwin, John R.: Investigation of a Related Series of Turbine-Blade Profiles in Cascade. NACA RM L53G15, 1953.
7. Whitney, Warren J., Buckner, Howard A., Jr., and Monroe, Daniel E.:
Effect of Nozzle Secondary Flows on Turbine Performance as Indicated by Exit Survey of a Rotor. NACA RM E54B03, 1954.
8. Lieblein, Seymour, Schwenk, Francis C., and Broderick, Robert L.:
Diffusion Factor for Estimating Losses and Limiting Blade Loadings in Axial-Flow-Compressor Blade Elements. NACA RM E53D01, 1953.
9. Stewart, Warner L.: Investigation of Compressible Flow Mixing Losses Obtained Downstream of a Blade Row. NACA RM E54I20, 1954.

| Blade section camber angle, θ_c , deg | Air inlet angle, β_1 , deg | | | | | Solidity investigated, σ | | Range of angle of attack, α_1 , deg |
|--|----------------------------------|-----|-----|-----|-----|---------------------------------|-----|--|
| | 0 | -15 | -30 | -45 | -60 | 1.5 | 1.8 | |
| 65 | ✓ | ✓ | ✓ | | | ✓ | ✓ | 26 - 53 |
| 80 | ✓ | ✓ | ✓ | | | ✓ | ✓ | 32 - 62 |
| 95 | | ✓ | ✓ | ✓ | | ✓ | ✓ | 50 - 73 |
| 110 | | | ✓ | ✓ | | ✓ | ✓ | 55 - 80 |
| 120 | | | | | ✓ | | ✓ | 69 - 72 |



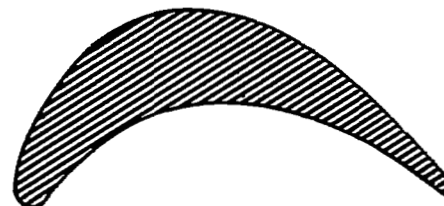
Primary turbine-blade section;
 θ_c , 65°; t/c, 10 percent



Primary turbine-blade section;
 θ_c , 110°; t/c, 15 percent



Primary turbine-blade section;
 θ_c , 80°; t/c, 10 percent



Secondary turbine-blade section;
 θ_c , 120°; t/c, 25 percent



Primary turbine-blade section;
 θ_c , 95°; t/c, 15 percent

1 Inch
|-----|

Figure 1. - Turbine-blade profiles and range of test conditions covered by low-speed two-dimensional cascade tests in reference 6.

| | Turbine design | | | |
|---|----------------|----------------|-----------------|----------------|
| | I (Ref. 2) | II (Ref. 3) | III (Ref. 4) | IV (Ref. 5) |
| Equivalent weight flow, $e \frac{w \sqrt{\theta_{cr}}}{\delta}$ | 11.95 | 11.95 | 11.95 | 11.95 |
| Equivalent work, $\frac{\Delta H}{\theta_{cr}}$, Btu/lb | 22.6 | 22.6 | 22.6 | 20.2 |
| Equivalent tip speed, $\frac{U_t}{\sqrt{\theta_{cr}}}$ | 597 | 597 | 597 | 597 |
| Mean-radius design diffusion parameter, D | 0 | 0.16 | 0.25 | 0.33 |
| Mean-radius solidity, σ | 2.85 | 2.81 | 2.36 | 2.16 |

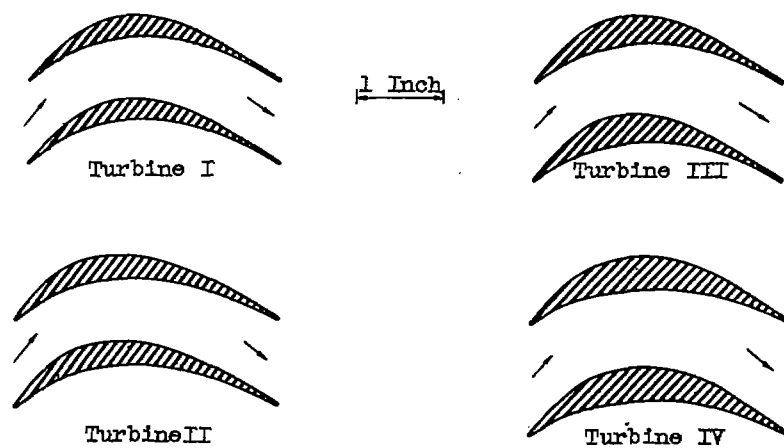


Figure 2. - Transonic turbine rotor mean-section blade profiles and flow passages and comparison of design features. (Same stator used on all turbines.)

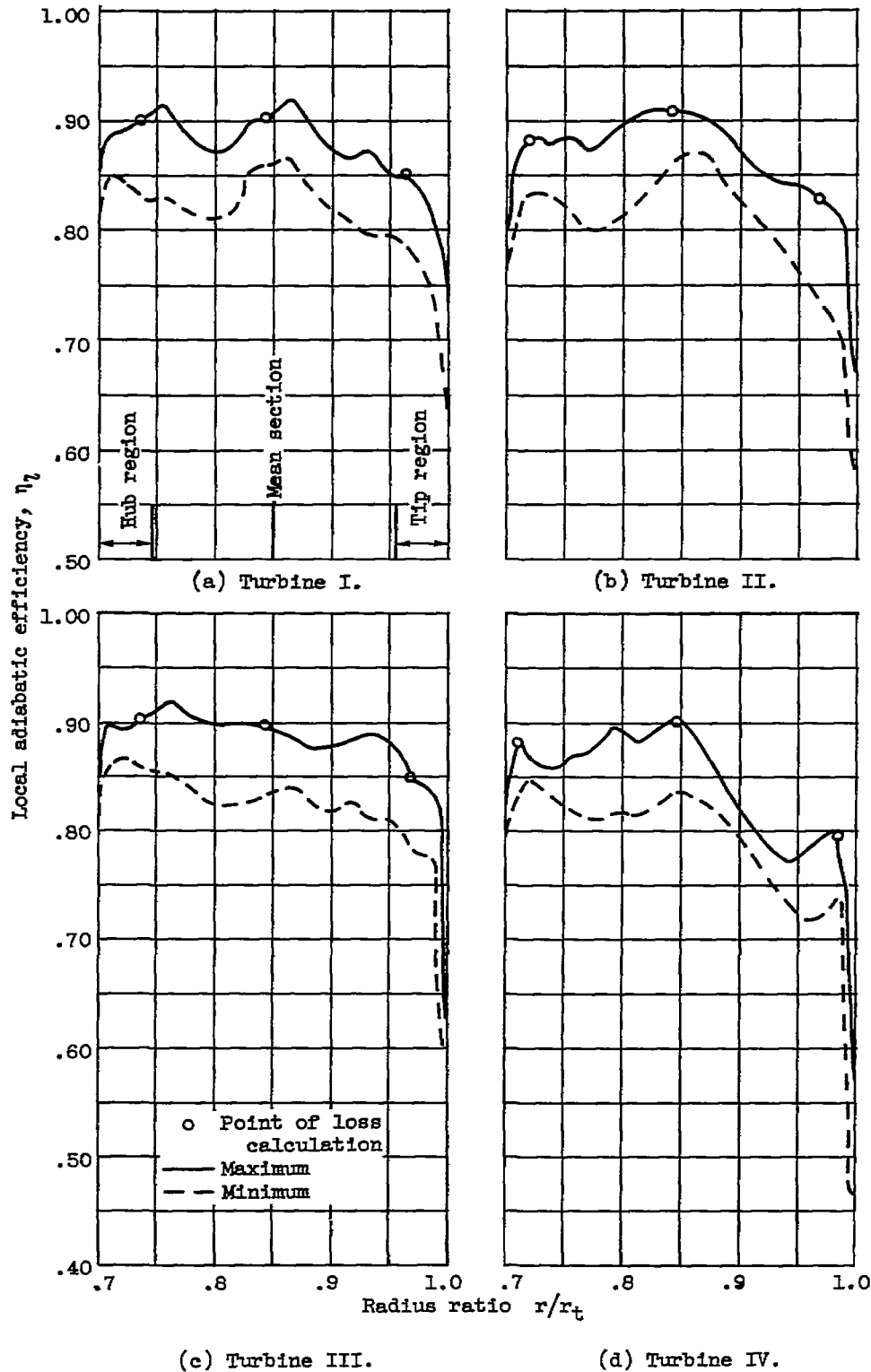


Figure 3. - Variation of maximum and minimum local adiabatic efficiency with radius for four transonic turbines.

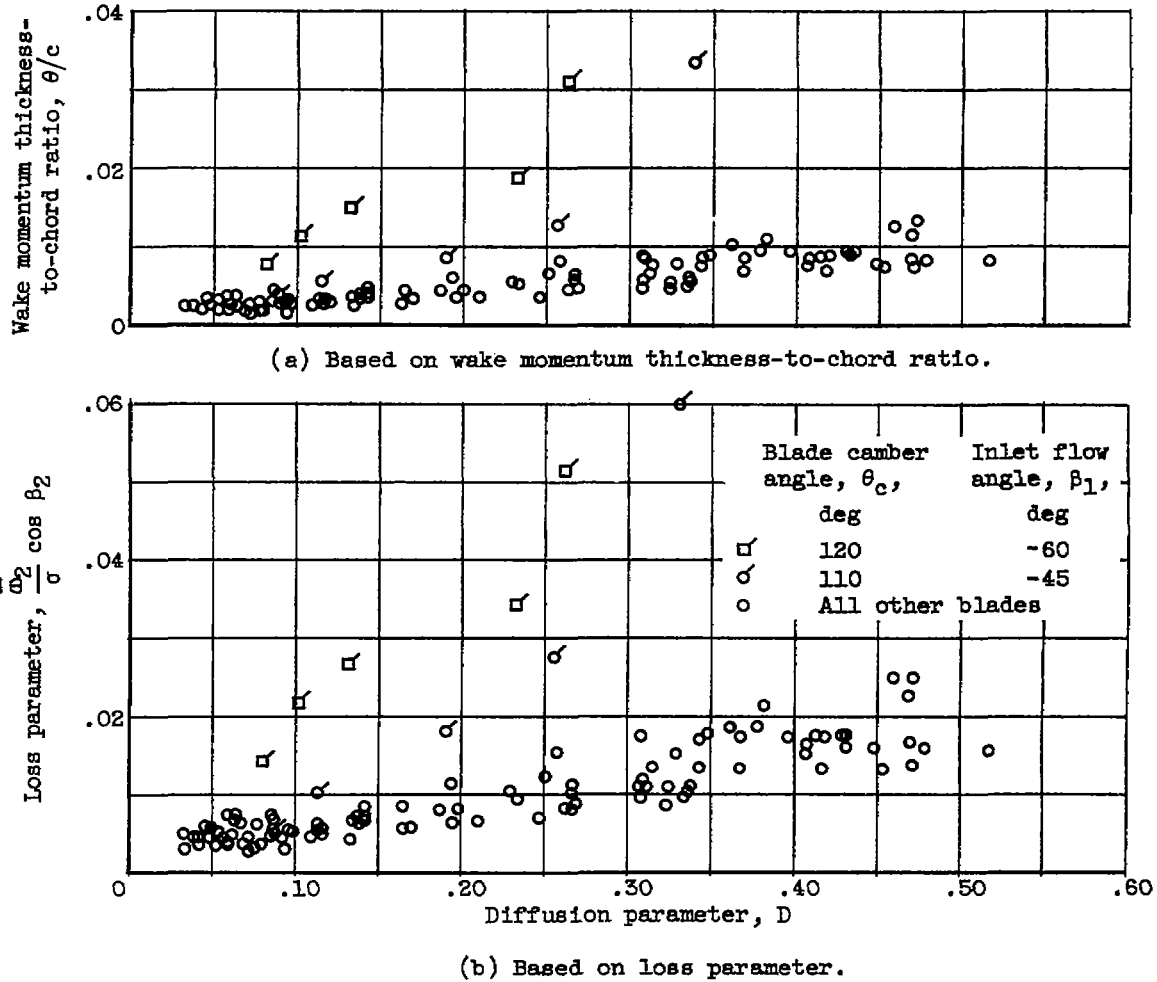


Figure 4. - Variation of loss with diffusion parameter for series of low-speed turbine blades in two-dimensional cascade.

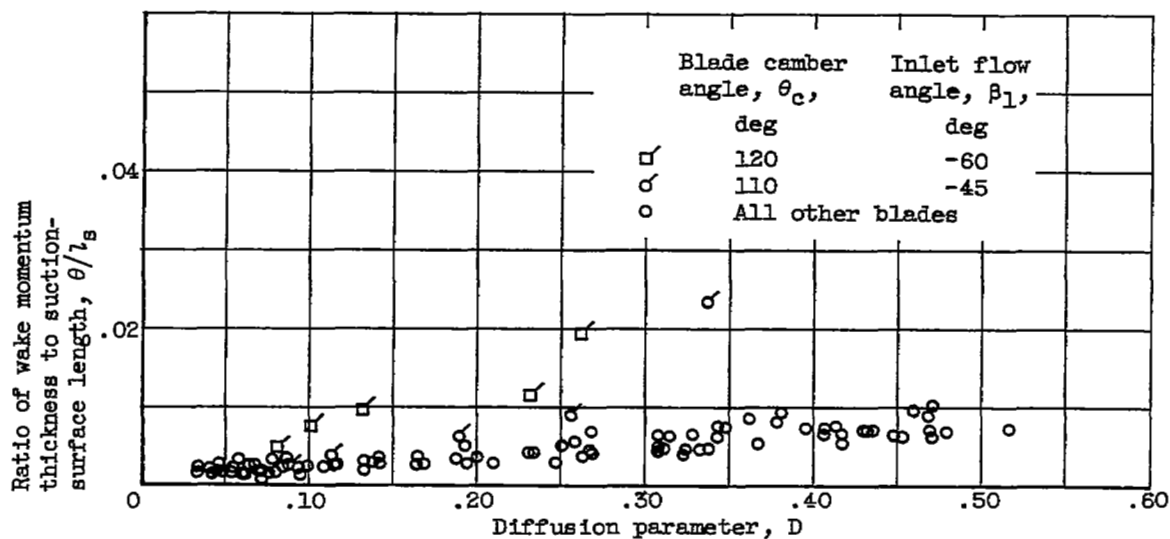


Figure 5. - Variation of ratio of wake momentum thickness to suction-surface length with diffusion parameter for a series of low-speed turbine blades in two-dimensional cascade.

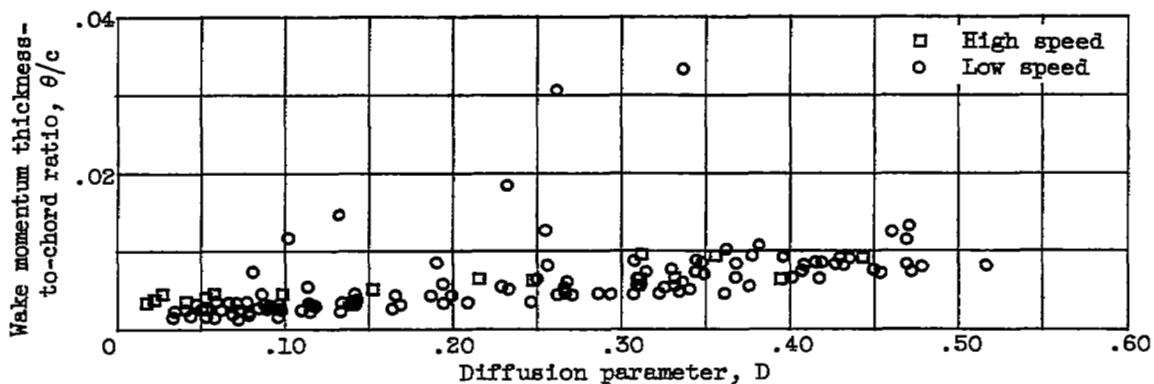


Figure 6. - Variation of wake momentum thickness-to-chord ratio with diffusion parameter for turbine blades in two-dimensional cascade obtained from limited high-speed tests and extensive low-speed tests (ref. 6).

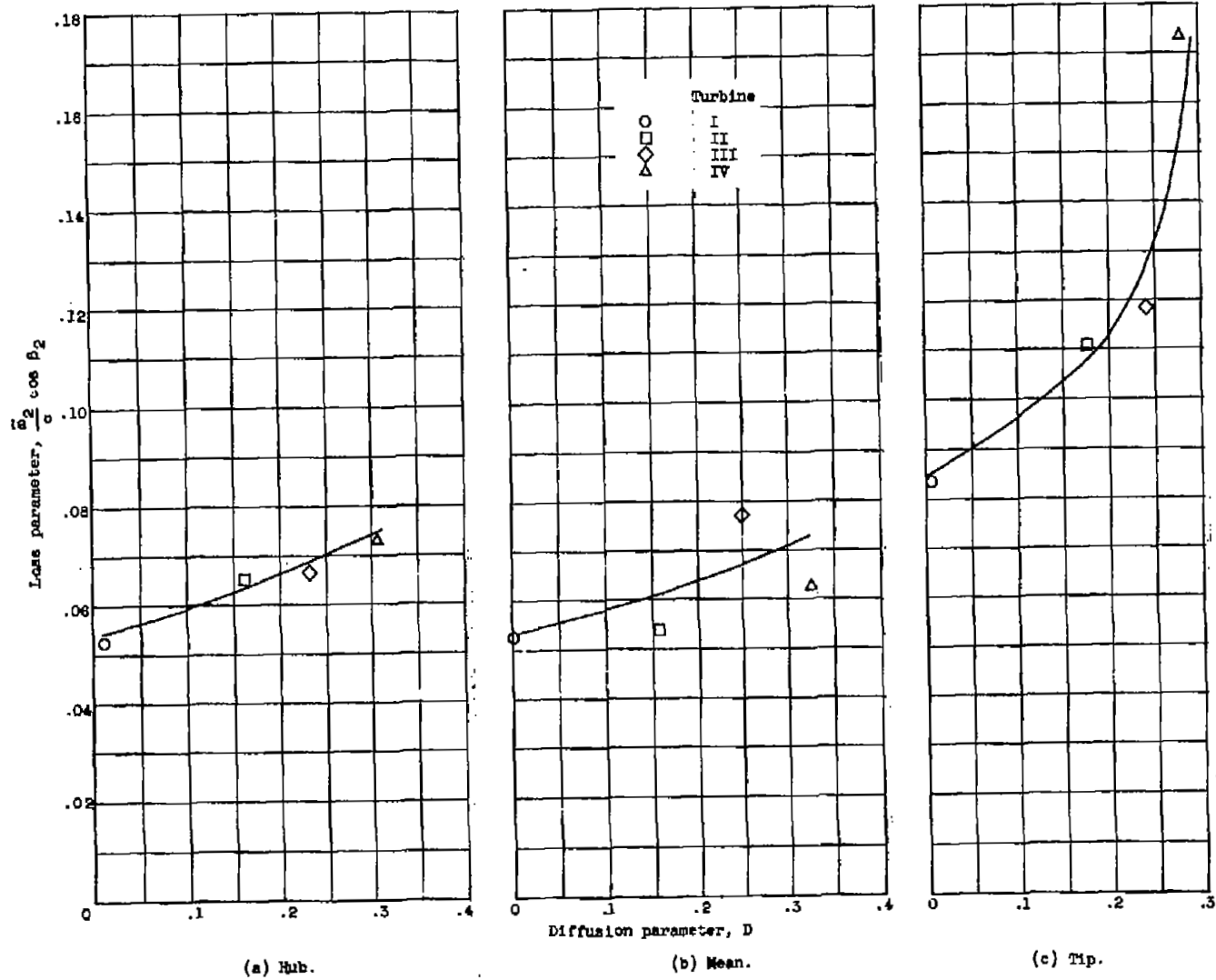


Figure 7. - Variation of measured blade-element loss parameter with design diffusion at hub, mean, and tip radius for four transonic turbines.

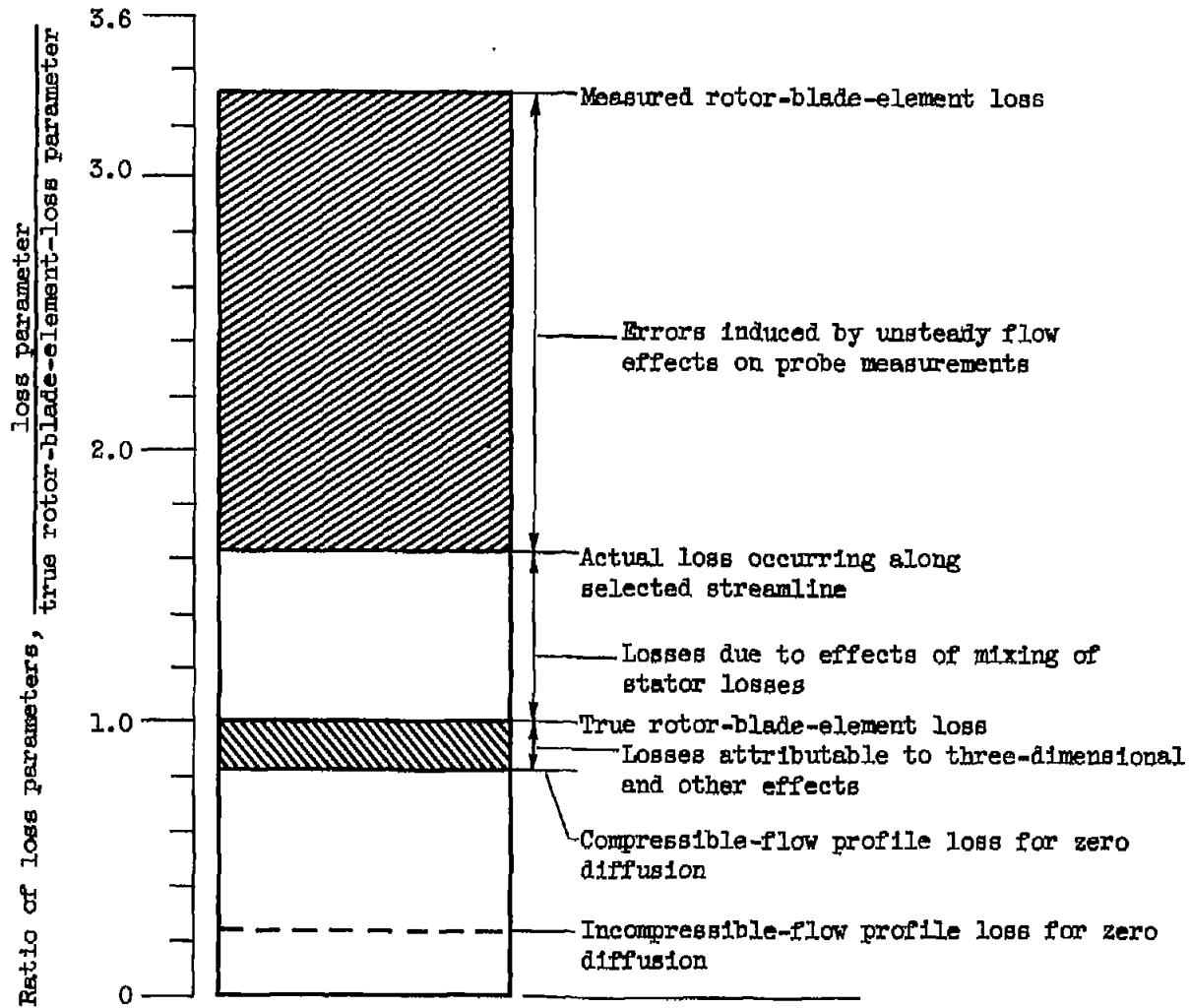


Figure 8. - Breakdown of losses indicated by local survey measurements at mean radius of turbine I.



NASA Technical Library
3 1176 01435 8080

1
1

1

1
1

